

13th EUROPEAN ROTORCRAFT FORUM

12.5

PAPER No. 50

**THEORETICAL AND EXPERIMENTAL DETERMINATION OF
THE ELASTIC AND INERTIAL PROPERTIES OF
AN HELICOPTER BLADE**

M. POUILLOT

AEROSPATIALE HELICOPTER DIVISION
MARIGNANE - FRANCE

P. SAVEL

AEROSPATIALE, C.E.H.B.
LE BOURGET, FRANCE

September 8 - 11 , 1987

ARLES , FRANCE

THEORETICAL AND EXPERIMENTAL DETERMINATION OF THE ELASTIC AND INERTIAL PROPERTIES OF A HELICOPTER BLADE

M. POUILLOT

AEROSPATIALE, MARGNANE

P. SAVEL

AEROSPATIALE, LE BOURGET

INTRODUCTION

A rotor dynamics programme named AFARP 6 (Anglo-French Aeronautical Research Programme) set up between Westland and Aérospatiale allowed grouping various operations meant to increase the efficiency of a number of research actions.

The validation of theoretical and experimental methods used to determine the elastic and inertial properties of helicopter blades was suggested as a specific theme within the framework of this bilateral cooperation programme.

The research work completed by Aérospatiale was applied to the Gazelle helicopter blade. This is a composite blade of conventional technology but designed along already dated concepts and it was felt indispensable to recharacterize this blade with the latest knowledge of materials and the computation methods currently used ; these previsional computation methods are briefly introduced at the beginning of this paper.

The experimental approach was original in the sense that strain gauges were used to determine properties of blade sections stressed in bending mode. The second part of the expose is therefore devoted to testing equipment and discusses, in particular, parasitic effects that may alter measurements as well as the solutions adopted to improve results accuracy after some fundamental research work.

Since the number of data acquired can be quite high, a method of measuring data analysis is described. This method involves solving a multidimensional calibration problem with confidence intervals where the various sources of error e.g. influence of noise on measurements or theoretical inadequacy are considered.

The expose ends with a description of the test method used to determine the blade torsional properties.

It is concluded that comparing calculation results and confronting these with experience shows how advanced previsional and test methods really are and how to pursue their development.

1 – THEORETICAL WORK

Defining helicopter blades is an iterative process calling on different disciplines. Repetitive computations are required in various fields (mechanical, loading, dynamic, stress and other characteristics) ; these computations are continued until the specifications (weight, service life, costs, etc ...) have been met.

Aérospatiale's Helicopter Division had initially developed separate computation codes. Stresses and limitations were thus determined from elastic and inertial characteristics, themselves derived with analytical methods implemented in the P2CARA code.

To simplify these operations and reduce engineering lead-times, the CHAMAIN code was developed with the help and support of Ecole Nationale Supérieure de l'Aéronautique et de l'Espace ; this code helps determine for a composite blade section :

- the equivalent beam's bending characteristics (flap and drag rigidity, position of neutral centre, angle of main inertia axis, rotor dynamics' mathematical integrals),
- the equivalent beam's torsional characteristics (rigidity and centre of torsion),
- stress levels under the effect of bending and torsional moments as well as shearing loads.

Although this equivalent characteristics' calculation problem has been well defined for homogeneous beams, it is proving significantly more difficult for composite beams, the linear sections of which are made of anisotropic materials with complex borders.

This problem has been overcome in the CHAMAIN code with a warping function [1, 2]. The equivalent beam's behaviour is defined with equilibrium equations and limit conditions.

These equations could directly be solved with analytical and integral methods or by finite differences. To make the nume-

rical solution easier to find, whatever the linear section's shape and composition may be, it has been preferred to consider this problem as a minimization solved with the bidimensional finite elements method. The latter only required bidimensional meshing, thus shortening design and computation time when compared to a general tridimensional method.

Because of this improvement in theoretical previsional methods and experimental comparison possibilities, it was thought appropriate to assess the resources currently available to orientate future research. This is one of the themes covered in cooperation between Aérospatiale and Westland Helicopters Ltd.

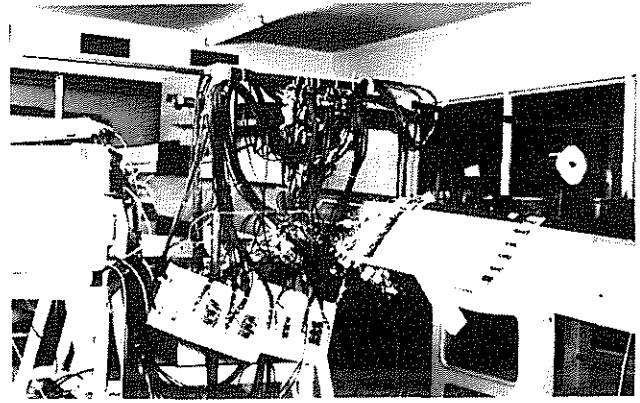


Fig. 1

Secondary measurements are made with clinometers, inclinometers and laser cells to determine angular variations as well as bending and torsional deflection (see Figure 2).

2 – RESEARCH ACTIVITIES DESCRIPTION

2.1 – GENERAL

2.1.1 – Programme of studies

The present study is divided into 3 parts [3] :

- Measuring equipment used for tests ; parasitic effects that may alter measurements and solutions adopted to minimize, if not cancel, these undesirable parasitic effects,
- Procedure applied to determine blade properties in bending mode ; comparison of theoretical and experimental results,
- Experiments with blade in torsion mode and comparison of results with theoretical predictions.

2.1.2 – Parameters quantified

The blade section characteristics that have to be determined experimentally are recalled below :

- Flapwise bending stiffness EI_B ,
- Chordwise bending stiffness EI_T ,
- Position of neutral centre CN,
- Angle α of the main inertia axis compared to reference axis,
- Torsional stiffness GJ ,
- Position of torsion centre CT and shear centre CC.

2.1.3 – Test configuration

Experiments were performed with a 7800 flight hours blade P/N 341A11-0040-00, S/N 133.

Measurements were made with 350Ω VISHAY UW 500 strain gauges.

The processing system used is an Analog Device (MACSYM 350) computer recording data simultaneously on every measuring channel ; this computer also allows immediate data processing (see Figure 1).

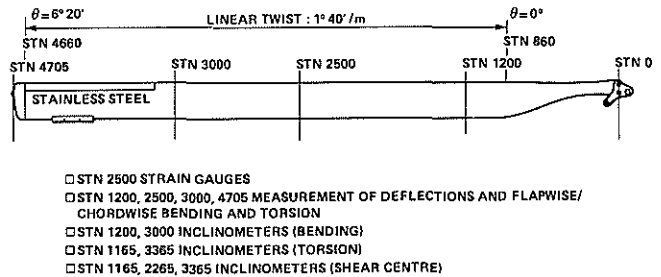


Fig. 2 : SA 341 HELICOPTER MAIN ROTOR BLADE

2.1.4 – Blade testing equipment

The blade section equipped for tests is in station 2500 (main section with polyurethane leading edge) ; this section is equipped with 38 gauges (see Figure 3) including :

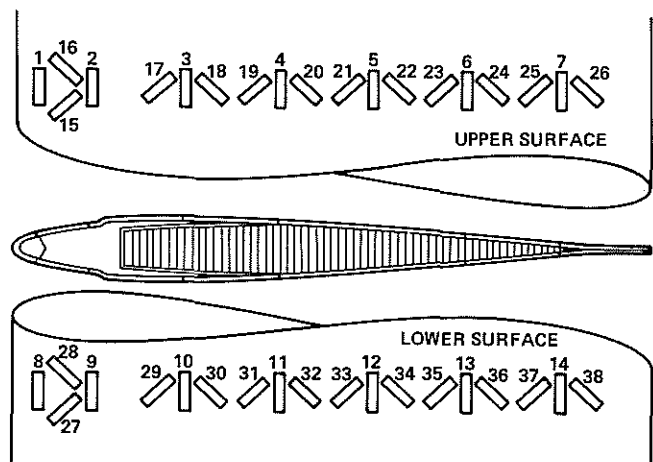


Fig. 3 : STRAIN GAUGES EQUIPMENT

- 14 gauges along the blade's centreline ; these will determine bending properties (EI_B , EI_T , CN, α).
- 24 gauges oriented $\pm 45^\circ$ to the blade's centreline ; these will record torsional deformations.

2.2 – MEASURING EQUIPMENT

2.2.1 – Reminder

Bending properties are determined from elongations measured under load on the periphery of the blade section considered. These elongations are related to gauges' resistance variations measured with a Wheatstone bridge. Different measurement configurations (full, half and quarter Wheatstone bridge) are available and to these correspond 4, 2 and 1 active gauges respectively. The configurations selected for testing purposes are substantiated in Paragraph 2.2.3.1.

2.2.2 – Measuring instruments

As mentioned in Paragraph 2.1.3. above, measuring data are acquired with a computer and stored in digital form. Results are processed directly to determine bending properties.

2.2.3 – Measurements alterations

Various parasitic effects may alter measurements. These effects are originally caused by composite materials making up the blade and supporting gauges. Composite materials are heterogeneous and characteristics may consequently change with external conditions e.g. temperature and humidity. Furthermore, measurements are made with strain gauges misadapted to laminates.

2.2.3.1 – Thermal effects

● Self-compensation

Self-compensating strain gauges should be used as far as possible i.e. these gauges should be designed in such a way that relative resistance variations are relatively horizontal over a definite temperature range for a given material.

Thermal compensation of a gauge generally calls for :

- structural expansion,
- gauge expansion,
- gauge wire resistivity.

The commercial gauges currently available are self-compensated for stable materials (stainless steel, steel, aluminium, etc ..) ; none exists as yet for composites.

A specific test was therefore performed in the oven on a 341 Gazelle blade element fitted out with 120Ω gauges self-compensated for tungsten (coefficient 03), steel (coefficient 06), and aluminium (coefficient 13). Figure 4 shows :

- some scattering of results for each gauge, thus confirming material heterogeneity,
- very poor self-compensation with aluminium strain gauges
- almost identical absolute self-compensation for tungsten and steel strain gauges.

Since no intermediate gauge is available between tungsten (03) and steel (06) ; steel gauges (06) were retained as the most varied and easily available.

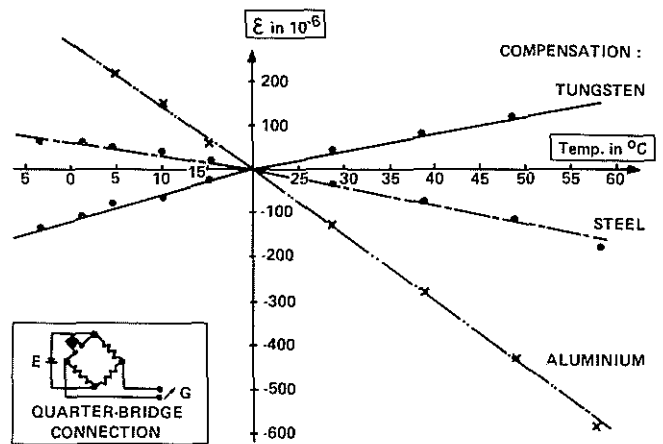


Fig. 4 : ELONGATION ϵ MEAN VALUES VERSUS TEMPERATURE T

● Half Wheatstone bridge configuration

It was previously mentioned that gauges cannot fully self-compensate for temperature because their resistance is not strictly constant, at least over a given range.

It has been noted that a 2 to 3°C variation induces a relative parasitic elongation from 5 to 10.10⁻⁶ for a quarter bridge connection.

The first step was then to perform the tests in a room air conditioned to 22 ± 2°C. The effects of those low temperature variations remained to be controlled.

A half Wheatstone bridge configuration was selected to exercise this control ; this configuration consists of (see Figure 5) :

- a measuring gauge on the blade,
- the adjacent gauge (compensating), on a measuring arm, on a section identical to the blade's and with the same chord abscissa,
- the remaining two gauges closing the bridge on a support adapted to self-compensation.

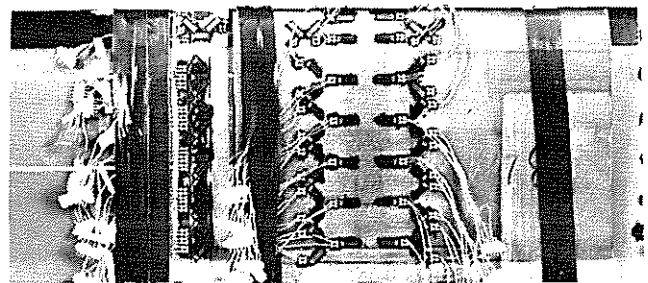


Fig. 5

It has been shown from the above that the effects of temperature are theoretically cancelled by identical resistance variations on both gauges of the Wheatstone bridge measuring arm.

This half bridge configuration was validated with additional equipment on a secondary 341 Gazelle blade element fitted out with 14 UW 500 gauges, 350 Ω and loaded into oven (see Figure 6).

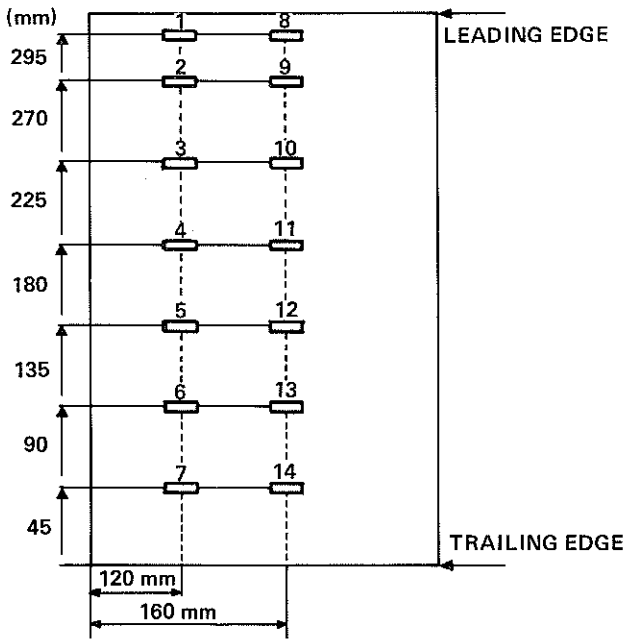


Fig. 6 : BLADE SECTION STRAIN GAUGES HALF BRIDGE CONNECTION EFFECTIVITY

Figure 7 shows that for a quarter bridge configuration with 40°C and 60°C temperature levels and gauge responses stabilized within ± 1 microdeformation, the effect of temperature on elongations is a function of the blade's internal structure. Hatched areas simulate the compensation to be obtained with a half bridge configuration.

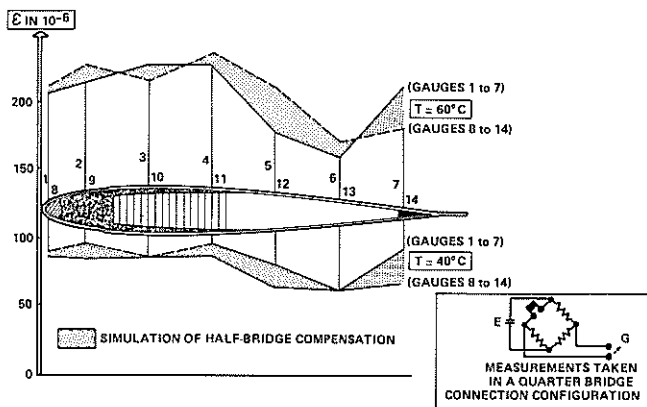


Fig. 7 : EFFECT OF TEMPERATURE T ON ELONGATIONS ϵ AS A FUNCTION OF INTERNAL STRUCTURE

Figure 8 compares results obtained with quarter and half bridge and shows that the latter configuration offers obvious advantages since measurements are centered with zero deviation and scattering is kept to a minimum.

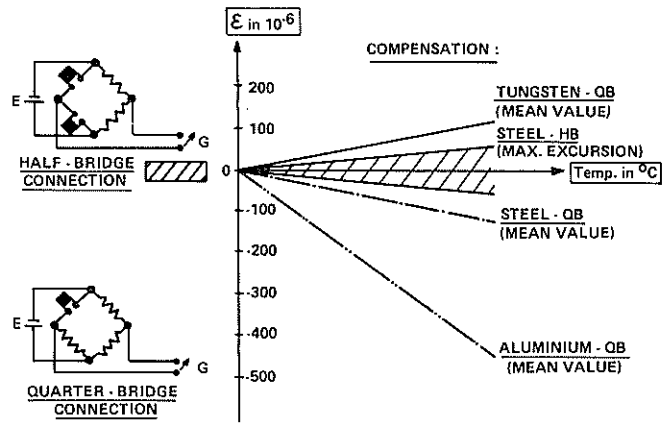


Fig. 8 : EFFECT OF HALF BRIDGE CONNECTION

2.2.3.2 – Other parasitic effects

● Wiring resistance

Wiring resistances reduce the sensitivity on the response bridge and generate errors in the interpretation of this bridge's calibration.

Gauge resistance must be as high as possible to minimize errors.

● Thermal wasting

Thermal wasting for composite materials such as glass epoxy must remain below 0.03 W/cm². In comparison, this power amounts to 0.30 W/cm² for steel.

● Materials heterogeneity

A gauge integrates distortions along its active axis. As regards composites, one should be careful on the surface discontinuity phenomena whose size can be that of the smallest gauges.

The heterogeneity problem can be approached through :

- the selection of the gauge,
- a statistic measure processing (see Paragraph 2.3.3.3.).

● Materials viscoelasticity

Following a test performed with a 10 kg load at blade tip, a variation of 2 microdeformations only was noted after two hours for an initial elongation of roughly 150 to 200 microdeformations. It was concluded from this test that the gauges are not very sensitive to viscoelastic phenomena on the Gazelle blade.

● Selection of gauges

These problems were solved with 350 Ω gauges 12.7 x 4.57 mm. This choice is a compromise decided after specific test between :

- insensitivity to local discontinuities,
- positioning accuracy,
- ease of implementation,
- acceptable thermal wasting.

2.3 – BENDING PROPERTIES

2.3.1 – General

It is reminded that the goal here was to determine the EI_B , EI_T , CN (Y_N and Z_N coordinates) and the α (Paragraph 2.1.2 refers) properties of a blade section from the elongation response curves of 14 longitudinal gauges while considering the test configurations as a whole. The conclusions are that 5 physical constants are to be determined ; these physical constants correspond to a number of data equal to :

$$N = n \times m \times p$$

where :

- n is the number of gauges,
- m is the number of test configurations (positions of the blade),
- p is the number of loadings per configuration.

2.3.2 – Theoretical reminders

According to Figure 9A, a number n of gauges (14 in this case) are positioned at points P_i ($1 \leq i \leq n$) on the periphery of a blade section.

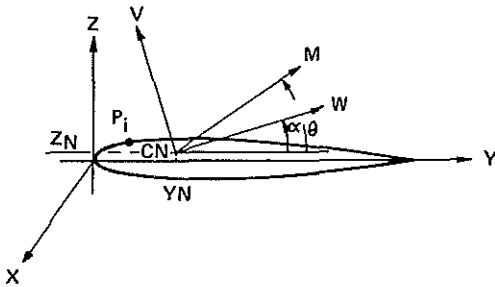


Fig. 9A

With M as the module of the moment applied and θ as its argument, the fundamental bending equation expresses standardized elongation λ_i (at points P_i) as a function of the 5 unknown variables to be determined :

$$\lambda_i = \frac{\epsilon_i}{M} \quad \epsilon_i: \text{ relative elongation in } P_i$$

$$= \cos(\theta - \alpha) [(Z - Z_N) \cos \alpha - (Y - Y_N) \sin \alpha] / (EI_B)$$

$$- \sin(\theta - \alpha) [(Y - Y_N) \cos \alpha + (Z - Z_N) \sin \alpha] / (EI_T)$$

The method of solution suggested by M. Morel, H.M. Mejean and R. Beraud from Marseille - Luminy University [4] involves first of all changing variables :

$$\begin{aligned} X_1 &= \cos \alpha & X_2 &= \sin \alpha \\ X_3 &= Y_N & X_4 &= Z_N \\ X_5 &= 1/EI_B & X_6 &= 1/EI_T \end{aligned}$$

Since the bending equation is standardized to the moment applied, the problem is how to solve the extra ($r \times 5$) equations ($r = n \times m$) with 5 unknown variables following :

$$\lambda_j = \sum_{k=1}^5 A[j, k] \cdot t_k \quad 1 \leq j \leq r$$

with :

$$t_k = f(X_i) \quad 1 \leq k \leq 5$$

In the least squares method, column matrix $T = (t_1, t_2, t_3, t_4, t_5)$ is the solution to the five linear equations with five unknown variables :

$$[A^t \cdot A] \cdot T = A^t$$

Unknown variables X_i , are consequently derived from :

$$X_k = \varphi_k(T)$$

2.3.3 – Confidence intervals

2.3.3.1 – Relations between λ_j and X_k statistics

Considering :

$$M = [A^t \cdot A]^{-1} \cdot A^t$$

$$= \text{matrix } (5, r)$$

variables t_k are expressed as :

$$t_k = \sum_{j=1}^r M(k, j) \cdot \lambda_j$$

Since there is some inaccuracy with standardized elongations λ_j , it is reasonable to assume that λ_j measurements are aleatory variables distributed in accordance with Gauss Law :

$$\text{Prob}(a \leq \lambda_j \leq b) = \frac{1}{\sigma_j \sqrt{2\pi}} \int_a^b e^{-\frac{(t - m_j)^2}{2\sigma_j^2}} dt$$

If mean m_j and standard deviation σ_j of random variable λ_j are assumed to be known (see Paragraph 2.3.3.3 below), it is demonstrated that random variables t_k follow the Gauss Law of parameters

$$m_{t_k} = \text{mean of } t_k = \sum_{j=1}^r M(k, j) \cdot m_j$$

$$\sigma_{t_k}^2 = \text{variance of } t_k = \sum_{j=1}^r M^2(k, j) \cdot \sigma_j^2$$

This relation presupposes that two measurements, λ_j and $\lambda_{j'}$, are not correlated.

Since :

$$X_k = \varphi_k(T)$$

a Taylor expansion close to (m_{t1}, \dots, m_{t5}) gives :

– the mean of 1st order variable X_k :

$$m_{X_k} = \varphi_k(m_{t1}, \dots, m_{t5})$$

calculated as the extra equations of Paragraph 2.3.2. were solved,

– the variance of 1st order variable X_k :

$$\sigma_{X_k}^2 = \sum_{i=1}^5 \left[\frac{\partial \varphi_k}{\partial t_i} \right]^2 \sigma_{t_i}^2$$

2.3.3.2 – Confidence intervals

Confidence intervals are given for each of the blade section characteristics ($EI_B, EI_T, Y_N, Z_N, \alpha$) by the Bienaymé-Tchebychev inequality :

$$\text{Prob} (|X_k - m_{X_k}| > \beta) < \frac{\sigma_{X_k}^2}{\beta^2}$$

where β is the maximum measurement inaccuracy for X_k .

2.3.3.3 – Statistical (m_j and σ_j) values of λ_j

Standardized elongation inaccuracies are caused by two factors :

- measurement inaccuracies,
- model inaccuracies.

1. Measurement inaccuracies

For each gauge and blade incidence is determined :

- a mean standardized elongation b_j corresponding to the gradient of elongations ϵ regression line as a function of applied moments M (see Figure 9B) ; this mean standardized elongation is determined as follows :

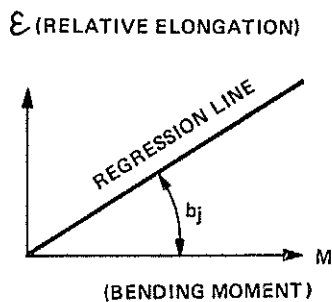


Fig. 9B

$$b_j = \frac{\text{cov}(M, \epsilon_j)}{\text{var}(M)} = \frac{\sum M \epsilon_j - \frac{\sum M \sum \epsilon_j}{p}}{\sum M^2 - \frac{(\sum M)^2}{p}}$$

– standard deviation σ_{b_j} associated to b_j :

$$\sigma_{b_j} = \frac{\sigma_{\epsilon_j} \sqrt{1-R^2}}{\sigma_M \sqrt{p-2}}$$

with :

$$\sigma_{\gamma}^2 = \frac{\sum \gamma^2 - \frac{(\sum \gamma)^2}{p}}{p-1} \quad R = b_j \frac{\sigma_M}{\sigma_{\epsilon_j}} \quad \gamma = \epsilon_{j,M}$$

2. Model inaccuracies

Whenever elongations calculated with experimental characteristics ($EI_B, EI_T, Y_N, Z_N, \alpha$) do not match measured values, it can be stated that there is :

- either a model inaccuracy,
- or a systematic error.

This systematic error is detected with the Grubbs criterion cancelling those gauges for which the distribution of calculated error amongst theoretical values and the distribution of measured error of standardized elongation is not Gaussian. To make this gauge error independent of incidence angle θ , the errors detected as a function of θ are summed up algebraically for each gauge.

To quantify the model inaccuracy, its variance σ_e^2 is determined for each gauge by summing up, while following incidence angle θ of the blade (m positions), the square of deviations e , where :

$$\sigma_e = \frac{1}{m-1} \sum_{\theta_1}^{\theta_m} |e|^2$$

$$e = b_j - \lambda_c$$

$\lambda_c = \lambda$ determined from the 5 experimental bending characteristics of the blade.

2.3.3.4 – Blade characteristics statistics

Measuring and modelization errors are assumed to be independent, mean m_j and variance σ_j^2 of standardized elongations on each gauge are expressed as :

$$m_j = b_j$$

$$\sigma_j^2 = \sigma_e^2 + \sigma_{b_j}^2 \quad 1 \leq j \leq r$$

2.3.4 – Bending tests

2.3.4.1 – Measurements

Elongations around blade section periphery at station 2500 which is sollicitated in bending mode, are determined in the following sequence (see Figures 10 and 11) :

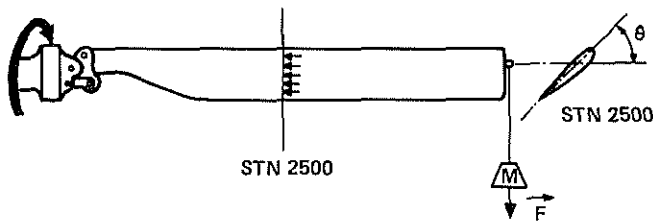


Fig. 10 : BENDING TEST

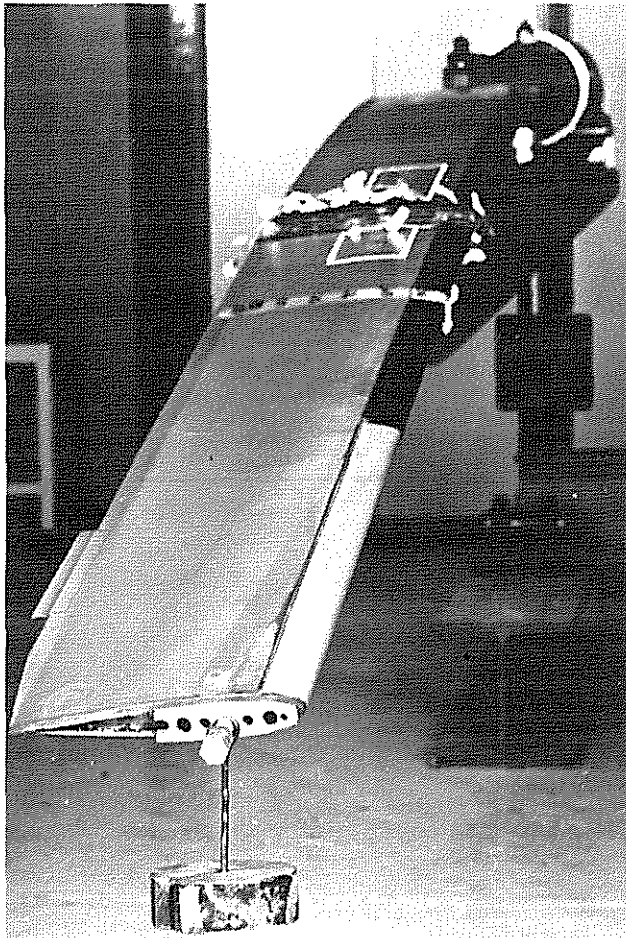


Fig. 11

- 14 longitudinal gauges ($n = 14$),
- 8 angles of incidence ($m = 8$) : $0^\circ, 45^\circ, 90^\circ, 135^\circ, 180^\circ, 225^\circ, 270^\circ, 315^\circ$,
- 10 loadings ($p = 10$) at blade tip,
- incidence variations recordings at stations 1200 and 3500,
- measurement of bending and torsional deformations at stations 1200, 2560, 3500 and 4700.

Confidence intervals are determined from 112 measurements ($r = n \times m$) processed.

Applying the Grubbs criterion shows that distributions of errors e (see Paragraph 2.3.3.3) is Gaussian in nature. Every gauge has been accounted for in the calculation of characteristics and their confidence intervals.

2.3.4.2 – Test results

Measurements made on blade section at station 2500 were processed with the following results :

- Experimental flap stiffness EI_B (6954 Nm^2) was determined within 1.15 % with 0.99 probability ; this stiffness is 5.47 % lower than the theoretical (7357 Nm^2) value (P2CARA code),
- Experimental drag stiffness EI_T (406065 Nm^2) was determined within 1.80 % with 0.99 probability ; this stiffness is 3.92 % higher than the theoretical (390765 Nm^2) value (P2CARA code),
- The following neutral center data were obtained :
 - Abscissa, with respect to leading edge :
 - Theoretical Y_N : 72.97 mm (P2CARA code)
 - Experimental Y_N : 74.76 ± 0.07 mm with 0.99 probability
 - i.e. a 2.45 % deviation with respect to theoretical value.
 - Ordinate, experimental values Z_N is 0.08 mm for zero theoretical value.
- The experimental angle of the main inertia axis is 0.04° with respect to the airfoil's symmetry axis ; theoretical value is zero.

2.4 – TORSIONAL CHARACTERISTICS

2.4.1 – General

Contrarily to those recorded in bending mode, torsional characteristics (GJ, CT, CC) are not derived from strain gauge measurements.

Because of the complex shape of the blade section and material anisotropy, there is no mathematical relation here comparable to the bending equation that would help determine physical properties from surface deformation measurements.

Elongation readings of the 24 gauges at $\pm 45^\circ$ were however recorded during torsion tests and memorized for later processing either to solve a direct problem with successive iterations or to solve a converse problem.

2.4.2 – Torsional stiffness

● **Fundamental relation**

Torsional stiffness GJ is determined experimentally by applying a pure torsional torque M_t to the blade and measuring the angular variation $\Delta\theta$ between two sections separated by a distance L , where :

$$GJ = \frac{M_t}{\Delta\theta / L}$$

● **Test configuration**

As shown on Figures 12 and 13, the blade is equipped with :

- 2 inclinometers at station 1200 and 3500,
- 2 clinometers at station 0 and 4700.

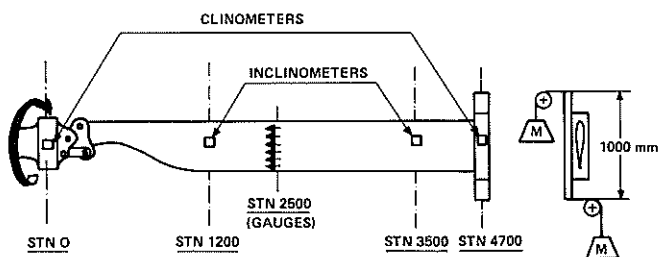


Fig. 12 : TORSIONWISE CALIBRATION - TEST SETUP

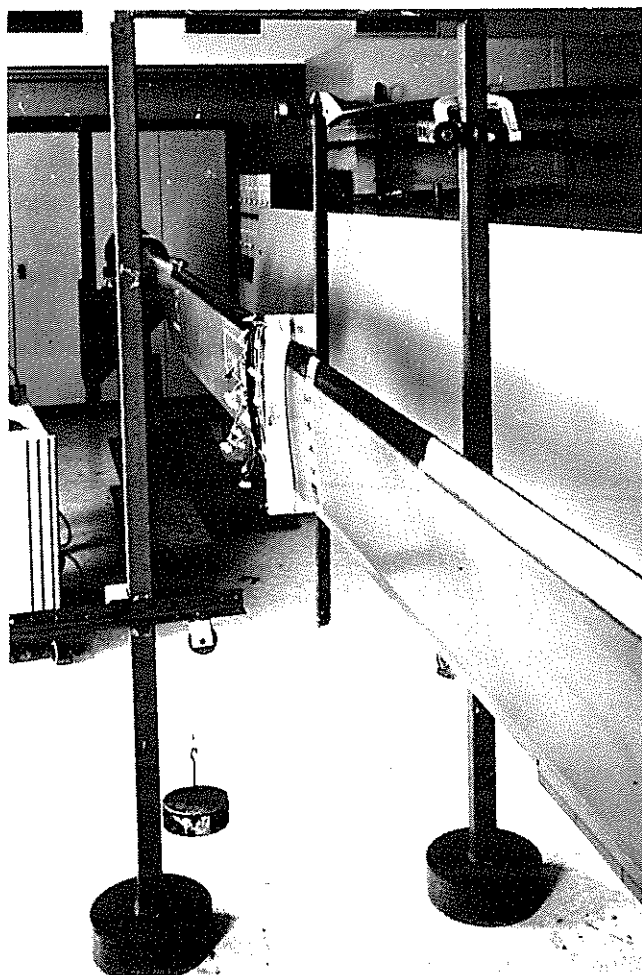


Fig. 13

The station 0 clinometer is meant to check that the recess does not pivot as the torque is applied or upon any correction.

The two inclinometers are 2.3 m apart for relative measuring accuracy. Inclinometers' and station 4700 clinometer's readings allow checking proper linearity of rotational variations in the blade's main section (non evolutive profile).

● **Test results**

Measurements proceed with the blade in a drag position to limit flap induced effects to a maximum.

Torques applied to the blade correspond to 12 loadings (6 nose-up and 6 nose-down).

Results have shown that :

- incidence variations recorded nose up or down have almost identical absolute values.
- application of a 98.1 Nm torsional torque produces an experimental torsional stiffness of 5620 Nm².

This latter value is 3.75 % below the theoretical (5839 Nm²) prediction (CHAMAIN code).

Elongation measurements for every ± 45° gauge (the most sensitive in torsional mode) are quite linear and gradients of regression lines are quite close, as absolute values, for a nose up and down torque.

2.4.3 – Shear centre

This characteristic is defined as the point where a shearing load applies without inducing a blade section rotation.

● **Test configuration**

The experimental procedure determining the shear centre is defined on Figures 14 and 15. The blade is fitted out with :

- 3 clinometers at station 1165, 2265 and 3365,
- 1 frame with a 2 m max. arm.

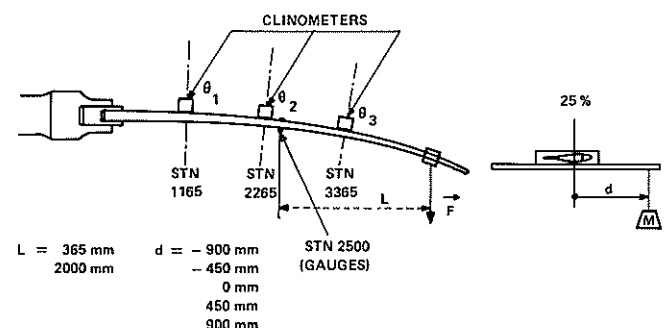


Fig. 14 : SHEAR CENTRE - TEST SETUP

The blade's main section is non evolutive. The distance separating the 3 clinometers allows for relative measuring sensitivity.

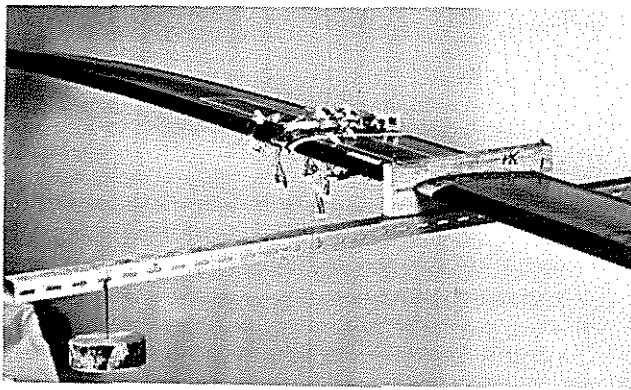


Fig. 15

● Test results

Measurements are made with the blade in a flap position and the blade section chord at station 2500 has a zero incidence.

Three loadings are applied at station 2865 and 4500 respectively for five different moment arms.

The shear centre is the point at which the three clinometers' readings are identical (recess may rotate) ; this centre is therefore determined graphically from test results.

Experimentally, the shear centre is 78 ± 27 mm aft of the leading edge.

2.4.4 — Centre of torsion

The centre of torsion of a blade section corresponds to the centre of rotation of that section subjected to a torsional moment.

Experimentally determining this specific point requires an ideal fit. To avoid damaging the blade, this test was performed on an available element fitted out with a stainless steel leading edge.

One element end in flapping position was recessed into a massive part.

Measurements were made 600 mm (2 chords) away from the recess to limit its influence.

A pure torsional torque was applied via a yoke positioned at the other blade end. The yoke/measured section distance was greater than the two chords.

Measurements were made with a tool especially designed to measure displacements of a blade section (see Figures 16 and 17) and compare with a reference section. Dial gauges only distinguish positional variations between measured section and reference section, any rotation of the recess that may occur would therefore not be recorded.

Figure 16 shows that the measurements made for each of the three moments of torsion applied are linear. The centre of torsion is the point of intersection of the three regression straight lines determined here. This point is 28.4 ± 2 mm away from the leading edge ; its theoretical value is 40.52 mm (CHAMAIN code) and its deviation is equivalent to 4.04 % of chord.

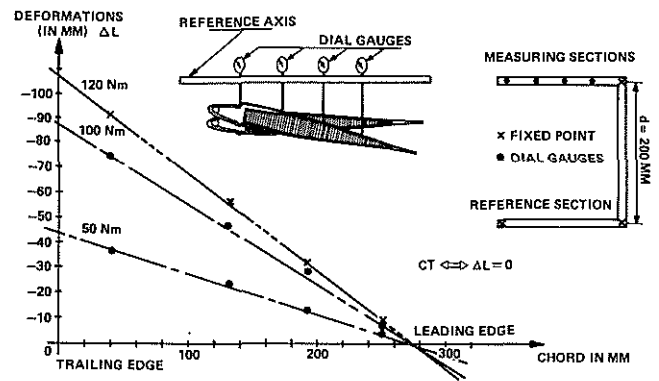


Fig. 16 : MEASURING SECTION ROTATION INDUCED BY A TORSIONAL TORQUE - DETERMINATION OF CENTRE OF TORSION

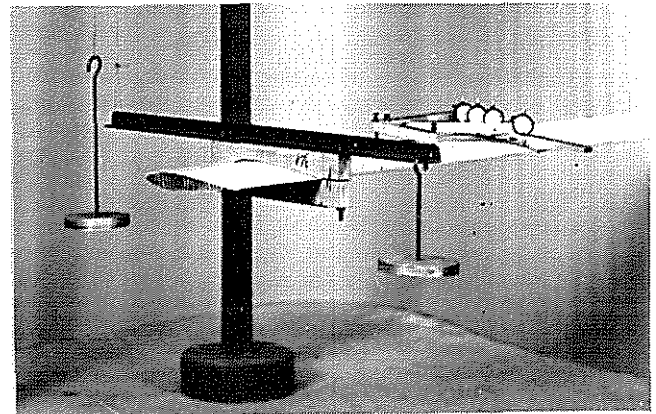


Fig. 17

3 — CONCLUSION

Theme No.1 of the Anglo-French Aeronautical Research Programme (AFARP 6) was the determination of helicopter blades' elastic and inertial characteristics.

Since the Gazelle blade type retained was designed some 15 years ago, it became necessary to redefine its theoretical mechanical characteristics from the material experience acquired and the provisional computation improvements made since then.

An original experimental approach was attempted by setting up 38 strain gauges at station 2500 of Gazelle blade S/N 133. A fundamental study allowed selecting 350Ω gauges 12.7×4.57 mm in a half Wheatstone bridge configuration to minimize parasitic effects.

As the elongation measurements were analyzed and processed directly with a MACSYM 350 computer, the bending characteristics of the blade's main section fitted out with a polyurethane leading edge were determined to be such that :

- the experimental flapping stiffness of 6954 Nm^2 determined within 1.15 % for an 0.99 probability is 5.47 % lower than the theoretical (7357 Nm^2) value (P2CARA code),

- the experimental drag stiffness of 406065 Nm^2 determined within 1.80 % for an 0.99 probability is 3.92 % higher than the theoretical (390765 Nm^2) value (P2CARA code),
- the experimental neutral centre abscissa is 74.76 mm away from leading edge i.e. a 2.45 % deviation with respect to the theoretical (72.97 mm) value (P2CARA code),
- compared to a zero theoretical deviation, the experimental angle of the main inertia axis to the airfoil symmetrical axis is of 0.04° .

Torsional characteristics were determined in a conventional manner but strain gauge measurements were memorized for later processing. It was proven that :

- experimental torsional stiffness is 5620 Nm^2 , 3.75 % lower than the CHAMAIN code's theoretical prediction of 5839 Nm^2 ,
- the experimental centre of shear is 78 ± 27 mm aft of the leading edge,
- the experimental centre of torsion is 28.4 ± 2 mm aft the leading edge (the CHAMAIN code's theoretical value is 40.52 mm).

It is generally demonstrated that bending and torsion correlations are quite satisfactory. However, some difficulty has been noted both by Aérospatiale and Westland, our British partners working on a Sea King blade, to determine the centre of shear.

These results will have to be compared to those obtained by WHL (computations and tests) as regards the Gazelle blade. This work will also be completed by a computation result analysis made by Aérospatiale on the one hand, and the computation and test results obtained by Westland on the other hand concerning the Sea King blade.

These researches will then allow obtaining conclusions which will qualify the current theoretical and experimental methods defined by the Anglo-French partners.

BIBLIOGRAPHY

- 1 J.J. BARRAU, D. GAY. «Calcul des caractéristiques équivalentes de torsion pour une poutre composite». First European Conference of Composite Materials, September 1985
- 2 G. MATHIEU. «Caractéristique d'une section de poutre composite. Introduction de l'effort tranchant» Document Aérospatiale/ENSAE
- 3 P. SAVEL. «AFARP 6 : Caractérisation expérimentale d'une pale 341». H/DE.R 48671
- 4 H. MOREL, H.M. MEJEAN, R. BERAUD. «Calcul des caractéristiques d'une section de pale d'hélicoptère et intervalles de confiance» Laboratoires API, Département Mathématiques-Informatique, Faculté de Luminy, MARSEILLE.